Enzymatic Catalyzed Synthesis and Triggered Gelation of Ionic Peptides

Jean-Baptiste Guilbaud,[†] Elisabeth Vey,[†] Stephen Boothroyd,[†] Andrew M. Smith,[†] Rein V. Ulijn,[‡] Alberto Saiani,[§] and Aline F. Miller*,[†]

[†]*School of Chemical Engineering and Analytical Sciences and Manchester Interdisciplinary Biocentre, University of Manchester, 131 Princess Street, Manchester M1 7DN, U.K.,* [‡]*WestCHEM, Department of Pure and Applied Chemistry, Strathclyde University, Glasgow, U.K., and* [§]*School of Materials, University of Manchester, Grosvenor Street, Manchester M1 7HS, U.K.*

We investigate the possibility of using the protease thermolysin to drive the synthesis and gelation of ionic-complementary peptides from nongelling precursors. In this system, short peptide fragments are continuously interconverted to form a dynamic peptide library, which eventually favors synthesis of peptides that are thermodynamically stabilized by molecular self-assembly. Thermolysin was added at a fixed concentration (0.3 mg mL^{-1}) to solutions (0−300 mg mL^{-1}) of the short tetrapeptide FEFK. Initially, the protease partially hydrolyzed the tetrapeptide into dipeptides in all samples. Subsequently, longer peptide sequences were found to form through reverse-hydrolysis. The stability of the different sequences was found to be dependent on their self-assembling properties. The sequences that self-assembled into antiparallel β-sheet rich fibers became the stable products for the reverse hydrolysis reaction, while the others formed were unstable and disappeared with increasing incubation time. Ultimately, the main product of the system was octapeptide, which suggests that it represents the thermodynamically favored product of this dynamic library. Its concentration dictated the gelation behavior of the sample, and gels with moduli up to 25 kPa where obtained depending on the initial concentration of tetrapeptide.

Introduction

Stimuli-responsive materials have received considerable attention recently owing to their potential biomaterials applications in, for example, drug delivery,[1−4] biosensing,[5] or regenerative medicine.[3,6−9] In this context the choice of building block is essential to allow the design of structures with controlled geometry and properties. While such supramolecular structures are traditionally fabricated from high molecular weight amphiphilic polymers, proteins and peptides have emerged as alternative building blocks as these biodegradable materials are known to self-assemble into ordered supramolecular architectures. Being able to trigger the self-assembly of these molecules by an external stimulus such as pH,[10−13] ionic strength,[14−17] or light[18] is attracting increasing attention as a route to control the reversible fabrication of novel soft-solid biomaterials. Motivation for this arises from the opportunities of incorporating protein-like responsiveness into the structure to provide temporal control over macroscopic properties and functionality.

Enzyme catalysis is one further class of stimuli that is known to induce changes in material properties.[19−25] Typically, enzymes have been used to hydrolyze materials, mainly polymers, for controlled drug delivery applications. Recently, however, enzymes have been exploited to trigger molecular assembly via reversed hydrolysis.[19,25,26] Examples for this latter method exploit a class of enzymes called proteases which are commonly known to hydrolyze peptide bonds. However, it has been shown that proteases can be encouraged to work in reverse when the reaction product is thermodynamically stabilized relative to its precursors. One interesting example involves the coupling of a nongelling

*To whom correspondence should be addressed. E-mail: aline.miller@manchester.ac.uk. Tel.: +44 (0) 161 306 5781. Fax: +44 (0) 161 306 4399.

(1) Hynd, M. R.; Turner, J. N.; Shain, W. *J. Biomater. Sci., Polym. Ed.* **2007**, *18*, 1223−1244.
(2) Aluri, S.; Janib, S. M.; Mackay, J. A. *Adv. Drug Delivery Rev.* **2009**, *61*, 940−952.
(3) Chung, H. J.; Park, T. G. *Nano Today* **2009**, *4*, 429−437.
(4) Wang, J.; Tang, F. S.; Li, F.; Lin, J.; Zhang, Y. H.; Du, L. F.; Zhao, X. J. *J. Nanomater.* **2008**, *8*, 516286.
(5) Hersel, U.; Dahmen, C.; Kessler, H. *Biomaterials* **2003**, *24*, 4385−4415.
(6) Gelain, F.; Horii, A.; Zhang, S. G. *Macromol. Biosci.* **2007**, *7*, 544−551.
(7) Baroli, B. *J. Pharm. Sci.* **2007**, *96*, 2197−2223.
(8) Horii, A.; Wang, X.; Zhang, S. *Nanotechnol. Tissue Eng., Scaffold* **2008**, 283−292.
(9) Peppas, N. A.; Sefton, M. V. *Advances in Chemical Engineering*; Academic Press: San Diego, CA, 2004; Vol. 29, p 234.
(10) Jayawarna, V.; Ali, M.; Jowitt, T. A.; Miller, A. E.; Saiani, A.; Gough, J. E.; Ulijn, R. V. *Adv. Mater.* **2006**, *18*, 611−614.
(11) Tang, C.; Smith, A. M.; Collins, R. F.; Ulijn, R. V.; Saiani, A. *Langmuir* **2009**, *25*, 9447−9453.
(12) Srivastava, A.; Ghorai, S.; Bhattacharjya, A.; Bhattacharya, S. *J. Org. Chem.* **2005**, *70*, 6574−6582.
(13) Pochan, D. J. *Nat. Mater.* **2009**, *8*, 773−774.
(14) Ozbas, B.; Kretsinger, J.; Rajagopal, K.; Schneider, J. P.; Pochan, D. J. *Macromolecules* **2004**, *37*, 7331−7337.
(15) Hong, Y.; Pritzker, M. D.; Legge, R. L.; Chen, P. *Colloids Surf., B* **2005**, *46*, 152−161.
(16) Basit, H.; Pal, A.; Sen, S.; Bhattacharya, S. *Chem.—Eur. J.* **2008**, *14*, 6534−6545.
(17) Cui, H. G.; Chen, Z. Y.; Zhong, S.; Wooley, K. L.; Pochan, D. J. *Science* **2007**, *317*, 647−650.
(18) Haines, L. A.; Rajagopal, K.; Ozbas, B.; Salick, D. A.; Pochan, D. J.; Schneider, J. P. *J. Am. Chem. Soc.* **2005**, *127*, 17025−17029.
(19) Yang, Z.; Liang, G.; Xu, B. *Acc. Chem. Res.* **2008**, *41*, 315−326.
(20) Dos Santos, S.; Chandravarkar, A.; Mandal, B.; Mimna, R.; Murat, K.; Saucede, L.; Tella, P.; Tuchscherer, G.; Mutter, M. *J. Am. Chem. Soc.* **2005**, *127*, 11888−11889.
(21) Adler-Abramovich, L.; Perry, R.; Sagi, A.; Gazit, E.; Shabat, D. *ChemBioChem* **2007**, *8*, 859−862.
(22) Ulijn, R. V.; Smith, A. M. *Chem. Soc. Rev.* **2008**, *37*, 664−675.
(23) Yang, Z. M.; Gu, H. W.; Fu, D. G.; Gao, P.; Lam, J. K.; Xu, B. *Adv. Mater.* **2004**, *16*, 1440−1444.
(24) Yang, Z. M.; Liang, G. L.; Xu, B. *Soft Matter* **2007**, *3*, 515−520.
(25) Yang, Z. M.; Xu, B. *Adv. Mater.* **2006**, *18*, 3043−3046.
(26) Toledano, S.; Williams, R. J.; Jayawarna, V.; Ulijn, R. V. *J. Am. Chem. Soc.* **2006**, *128*, 1070−1071.

N-(fluorenylmethoxycarbonyl) (Fmoc) amino acid to a dipeptide to create a Fmoc-tripeptide using proteases.[26−28] In dilute aqueous solutions hydrolysis of the peptide is favored; however, the equilibrium was found to shift in more concentrated systems in favor of the Fmoc−tripeptide synthesis as a further equilibrium favored the self-assembly of these molecules into nanofibrous structures driven by *π*-stacking. These fibers eventually became physically entangled and formed a hydrogel above a critical concentration. This example involved the use of poorly soluble peptide derivatives resulting in a suspension-to-gel transition upon the addition of enzyme. Such enzyme responsiveness is a particularly attractive hydrogel fabrication route as it is highly selective and occurs under mild conditions with water being the only byproduct.

Here we exploit the reverse hydrolysis method to synthesize ionic peptides (containing alternating charged and noncharged amino acids) that are well-known to self-assemble into *β*-sheet-rich fibrillar hydrogels. Such peptides are gaining increasing popularity in the literature because of their potential biomaterials applications and for aiding the understanding of the general paradigms that govern molecular self-assembly.[29−33] The key idea behind this is that we can start with a solution containing readily soluble, short, easy to synthesize peptides and simply use an enzyme to couple the precursor peptides together, which will result in a sol−gel transition and consequently a 3-dimensional matrix ready for biomaterials applications. This method opens up the possibility of synthesizing a diverse range of ionic peptides with no harsh chemicals in an aqueous environment. In addition this is a particularly attractive hydrogel fabrication route for 3D tissue engineering applications as it can be used to trigger gelation in the presence of cells resulting in the homogeneous incorporation of such cells throughout a biocompatible, 3D hydrogel matrix.

On the basis of Zhang's and our previous work with ionic peptides[29,31,34,35] we selected the tetrapeptide FEFK (F is phenylalanine, E is glutamic acid, and K is lysine, Figure 1), as this peptide does not form hydrogels at pH 7 in the concentration range investigated (0−300 mg mL^{-1}) while the related octapeptides FEFKFEFK and FEFEFKFK form hydrogels at low concentrations (10 and 15 mg mL^{-1}, respectively).[35] We have shown in our previous work that these two octapeptides form *β*-sheet-rich fibers at low concentrations, below the critical gelation concentration, CGC, and that above CGC the fibers self-associate/entangle to form self-supporting hydrogels.[35,36] The enzyme selected here was thermolysin from *Bacillus thermoproteolyticus rokko* as it is known to hydrolyze peptide bonds on the amino side of hydrophobic residues,[37] in our case F. The enzyme-triggered gelation of FEFK was investigated initially using
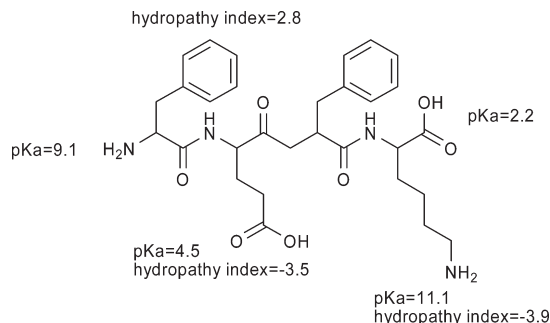

Figure 1. Formula of the tetrapeptide FEFK showing the pK_a and hydropathy index of the amino acid residues.

oscillatory rheometry as a function of time to confirm that a gel does indeed form and also to identify the critical gelation time. Subsequently matrix assisted laser desorption ionization−time-of-flight mass spectroscopy (MALDI-TOF MS) in conjunction with high performance liquid chromatography (HPLC) were used to both qualitatively and quantitatively characterize the peptide sequences synthesized at different time points. The development of the secondary structure of the peptide was monitored using time-resolved Fourier transform infrared (FTIR) spectroscopy and transmission electron microscopy (TEM).

Materials and Methods

Peptide Synthesis. All Fmoc-amino acids, activator (HCTU), Fmoc-Lys(Boc)-Wang resin were purchased from Novabiochem (Merck) and used as received. All other reagents and solvents were purchased from Aldrich and used without further purification. The tetrapeptide FEFK was synthesized via standard solid phase peptide synthesis on a ChemTech ACT 90 peptide synthesizer (Advance ChemTech, Ltd.) where each amino acid coupling step was confirmed using the Kaiser test. After cleavage from the resin and deprotection of the side groups and N-terminus using a TFA−anisole (95/5) mixture, the peptides were recovered and washed in cold ether, centrifuged, and freeze-dried. HPLC, MS, and ^{1}H NMR were used to confirm the peptide structure and estimate their purity. Di-, tetra-, hexa-, and octapeptides used to calibrate the HPLC data were also synthesized using the same procedure. All peptides synthesized were found to have a purity of ca. 90% where the impurities were predominantly shorter peptide sequences and residual TFA (<1%).

Sample Preparation. Thermolysin form *Bacillus thermoproteolyticus rokko* was purchased from Sigma-Aldrich and used as received. FEFK solutions with initial concentration, C_0, ranging from 40 to 300 mg mL^{-1} were prepared by dissolving the desired quantity of tetrapeptide in distilled water and adjusting the pH to 7 by adding a few drops of molar NaOH solution. At pH 7, the carboxylic acid and amine groups are in their basic and acidic state, respectively, and the tetrapeptide does not present a net charge (Figure 1). Thermolysin is subsequently added to each solution at a concentration of 0.3 mg mL^{-1}, and the solution was vortexed for 30 s. The resulting samples were used immediately for analysis.

Oscillatory Rheology. Rheological studies were undertaken on a strain-controlled Bohlin C−CVO rheometer with temperature control. Parallel plate geometry of 40 mm diameter was used with a 0.5 mm gap. A solvent trap was fitted to minimize evaporation. The frequency and the strain were fixed to 1 Hz and 1%, respectively. Samples were loaded directly on the stage and the elastic (G') and viscous (G'') moduli measured every 8 s for 2−12 h to monitor the sol−gel transition and the development of the hydrogels.

Reversed Phase-High Performance Liquid Chromatography (RP-HPLC). RP-HPLC analyses were conducted at 25 °C on an Ultimate 3000 HPLC system (Dionex) equipped with a variable

(27) Williams, R. J.; Smith, A. M.; Collins, R.; Hodson, N.; Das, A. K.; Ulijn, R. V. *Nat. Nanotechnol.* **2009**, *4*, 19−24.

(28) Das, A. K.; Hirst, A. R.; Ulijn, R. V. *Faraday Discuss.* **2009**, *143*, 293−303.

(29) Zhang, S. G.; Holmes, T.; Lockshin, C.; Rich, A. *Proc. Natl. Acad. Sci. U.S.A.* **1993**, *90*, 3334−3338.

(30) D'Auria, G.; Vacatello, M.; Falcigno, L.; Paduano, L.; Mangiapia, G.; Calvanese, L.; Gambaretto, R.; Dettin, M.; Paolillo, L. *J. Pept. Sci.* **2009**, *15*, 210−219.

(31) Zhang, S. G.; Lockshin, C.; Cook, R.; Rich, A. *Biopolymers* **1994**, *34*, 663−672.

(32) Caplan, M. R.; Schwartzfarb, E. M.; Zhang, S. G.; Kamm, R. D.; Lauffenburger, D. A. *Biomaterials* **2002**, *23*, 219−227.

(33) Schneider, J. P.; Pochan, D. J.; Ozbas, B.; Rajagopal, K.; Pakstis, L.; Kretsinger, J. *J. Am. Chem. Soc.* **2002**, *124*, 15030−15037.

(34) Boothroyd, S.; Saiani, A.; Miller, A. F. *Macromol. Symp.* **2008**, *273*, 139−145.

(35) Mohammed, A.; Miller, A. F.; Saiani, A. *Macromol. Symp.* **2007**, *251*, 88−95.

(36) Saiani, A.; Mohammed, A.; Frielinghaus, H.; Collins, R.; Hodson, N.; Kielty, C. M.; Sherratt, M. J.; Miller, A. F. *Soft Matter* **2009**, *5*, 193−202.

(37) Morihara, K.; Tsuzuki, H. *Eur. J. Biochem.* **1970**, *15*, 374−380.

wavelength UV detector (wavelength used 210 nm) and a gradient pump. Separation was performed on an Acclaim C18 analytical column (3 μm, 4.6 × 150 mm) fitted with a 300 Guard Cartridge (4.3 × 10 mm). A flow rate of 1 mL min^{-1} was used for all separations. The mobile phase consisted of a mixture of water: TFA(0.1%) and acetonitrile:TFA(0.1%). Aliquots of 20 μL were sampled at discrete time points and diluted 50 fold in a 4:1 water/ acetonitrile mixture before injecting 100 μL into the column using an ACC-3000 autosampler. Data were analyzed using Chromoleon 6.80 software.

Matrix Assisted Laser Desorption Ionization-Time of Flight Mass Spectroscopy (MALDI-TOF MS). MALDI-TOF MS analysis was performed on an Axima CFR mass spectrometer (Shimadzu Biotech) in reflectron positive mode using a nitrogen laser (337 nm). The matrix was prepared by dissolving ca. 0.1 g of α-cyano-4-hydroxycinnamoc acid (CCA) in 250 μL of acetonitrile before adding 25 μL of a 2% formic acid solution and 225 μL of HPLC grade water. A 20 μL portion of sample was diluted in 1 mL of HPLC grade water, and 1 μL of this sample was mixed with 1 μL of the matrix solution on a stainless steel sample plate. The plate was allowed to dry for ca. 10 min prior to analysis. All mass spectra were generated by collecting 100 laser shots, and laser strength was adjusted to obtain optimal signal-to-noise ratio. The data were analyzed using Kompact 2.4.1 software.

Attenuated Total Reflectance-Fourier Transform Infrared Spectroscopy (ATR-FTIR). Secondary structures of the peptides were determined using ATR-FTIR on a Thermo Nicolet 5700 spectrometer using a smart multibounce ARK accessory (Thermo Nicolet) with a zinc selenide crystal. A background spectrum of HPLC grade water was taken prior to any sample analysis and subtracted from all sample spectra. Samples were placed directly onto the crystal stage, and spectra were collected every 64 s for 10 h. Each spectrum was an average of 64 scans. OMNIC 7.2 software was used for data acquisition and processing.

Transmission Electron Microscopy (TEM). TEM data were recorded for samples at C_0 = 70, 100, and 200 mg mL^{-1} at discrete time points to monitor the formation of fibrillar structures. For C_0 = 70 mg mL^{-1}, samples were prepared without further dilution, for C_0 = 100 and 200 mg mL^{-1} samples prepared after 24 h of incubation were diluted 10-fold in water and agitated vigorously to separate fibrillar structures. Carbon-coated copper grids (no. 400, Agar Scientific) were glow-discharged for 30 s and placed shiny side down on the surface of a 10 μL droplet of sample for less than ca. 5 s. Absorbed grids were immediately placed on a 10 μL droplet of doubly distilled water for 30 s and blotted. Washed grids were then placed on a 10 μL droplet of freshly prepared and filtered 4% (w/v) uranyl acetate for 30 s for negative staining and then blotted continuously against Whatman 50 filter paper. Data were recorded in a Joel 1220 TEM operating at 100 keV and images were recorded using a Gatan Orius CCD camera at a specimen level increment of 2.9 Å pixel^{-1}.

Results and Discussion

As discussed in the introduction no gel was found to form using the "tilting test-tube method" for pure tetrapeptide FEFK (i.e.: with no added thermolysin) within the concentration range investigated: 0−300 mg mL^{-1}. Interestingly no significant increase in sample viscosity was observed either suggesting that this short peptide does not self-assemble in water at pH 7. In contrast, when 0.3 mg mL^{-1} of themolysin was added, clear, self-supporting hydrogels were obtained depending on the initial tetrapeptide concentration, C_0, and the incubation time, t_{inc} (Figure 2). For C_0 < 70 mg mL^{-1} samples remained in the liquid state even after several days of incubation. Samples with 70 < C_0 < 100 mg mL^{-1} exhibited an increase in viscosity, but still flowed upon inversion of the vial after 24 h. For C_0 > 100 mg mL^{-1} self-supporting hydrogels formed. The
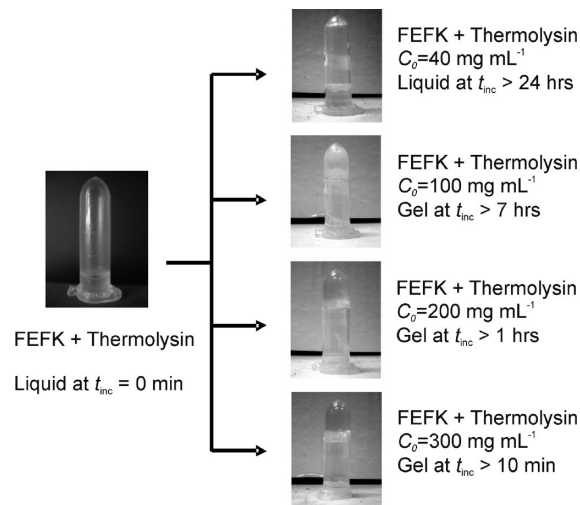

Figure 2. Optical photographs for 40, 100, 200, and 300 mg mL^{-1} samples showing their macroscopic appearance (solution/gel) before and after the addition of thermolysin (0.3 mg mL^{-1}).
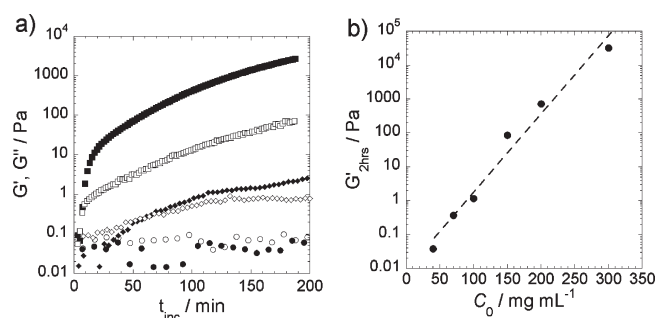

Figure 3. (a) Evolution of the storage, G', (closed symbols) and loss, G'', (open symbols) moduli of the 40 mg mL^{-1} (circle), 100 mg mL^{-1} (diamond), and 200 mg mL^{-1} (square) samples as a function of incubation time. (b) Sample storage moduli, G', after 2 h of incubation as function of the initial tetrapeptide concentration, C_0.

macroscopic gelation time, t_{mgel} (time at which the sample stopped flowing upon inversion of the vial), was found to decrease with increasing initial tetrapeptide concentration, and for C_0 = 300 mg mL^{-1} a self-supporting hydrogel was obtained after only 10 min.

The dynamics of the gelation process were followed using oscillatory rheology. In Figure 3a the evolution of the storage, G', and loss, G'', moduli for samples prepared with an initial concentration of tetrapeptide of 40, 100, and 200 mg mL^{-1} are presented as a function of t_{inc}, the incubation time. For C_0 = 40 mg mL^{-1} G'' was always larger, or of the same order of magnitude, than G' during the 3.5 h probed. Similar behavior was observed for aliquots of preprepared samples over significantly longer times, up to 24 h. This confirms our visual observations that samples remain in a liquid state at low C_0. Different behavior was observed when C_0 = 100 mg mL^{-1}. For t_{inc} < 60 min G'' was larger than G' indicating that the sample was in a liquid state, while for t_{inc} > 65 min G' was larger than G'' which is indicative of solid-like behavior typical of physically entangled fibrillar gels. For C_0 = 200 mg mL^{-1} G' was found to increase sharply during the first 20 min of incubation. The crossover point between G' and G'' was found at 6 min for this sample. The crossover point is often used to define the gelation time, t_{gel}. Not surprisingly considering the very different approaches used, t_{gel} and the macroscopic gelation time (obtained through the "tilting test-tube method"), t_{mgel}, are very different, the latter being larger.
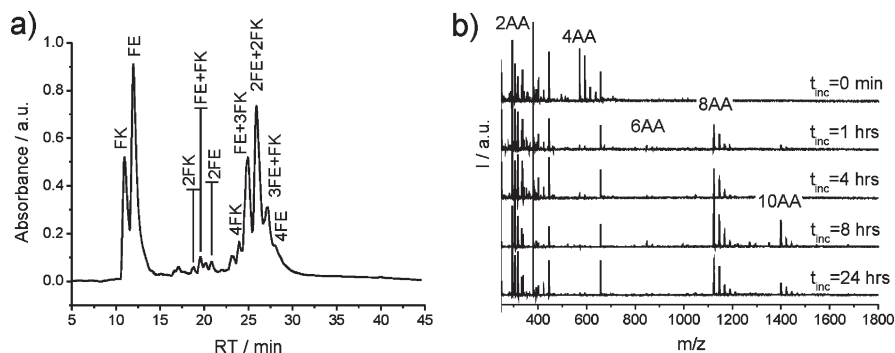
Figure 4. (a) HPLC chromatograph with sequence assignment for the 200 mg mL^{-1} sample incubated for 24 h; (b) MALDI-TOF mass spectra obtained at different incubation times for the 200 mg mL^{-1} sample with sequence assignment of the peaks.

When using oscillatory rheology the mechanical properties of the gels are probed using small shear stresses, which are thought to have minimal effect on the overall gel structure. t_{gel} is, therefore, thought to correspond to the point in time at which a percolated 3D network is present in the sample. On the other hand the "tilting test-tube method" involves the application of a relatively large shear force to the sample, which depends on the geometry and size of the test tube used. For weak gels this will result in a breakdown of the gel and consequently it will flow. From a practical perspective t_{mgel} is often more relevant as many applications require self-supporting hydrogels that can be handled easily. The samples' storage moduli after 2 h of incubation are given as a function of C_0 in Figure 3b. It is clear that G' is strongly dependent on C_0. For $C_0 = 300$ mg mL^{-1} a storage modulus of 25 kPa is obtained which is significantly larger than the storage moduli usually reported in the literature for ionic-complementary peptide-based hydrogels.[38]

MALDI-TOF MS and RP-HPLC were used to qualitatively and quantitatively monitor the composition of the samples at discrete time points after the addition of thermolysin. Reference chromatographs of pure di-, tetra-, hexa- and octapeptide sequences provided the range of retention times corresponding to the different species (10−13 min for dipeptide, 18−21 min for tetrapeptide, 21−23 min for hexapeptide, 23−27 min for octapeptide). To estimate the actual concentration of the octapeptides present in our samples, a calibration curve (concentration vs RP-HPLC peak area) using samples with known concentrations of FEFKFEFK and FEFEFKFK was established. The UV frequency used for the detection of the peptide species results in the RP-HPLC peak area being directly proportional to the concentration of peptide bonds present, and hence the specific sequential arrangement of amino acids does not affect the HPLC peak area or time. The overall hydrophobicity, on the other hand, does affect the elution time of the peptide species, where the more hydrophobic sequences (i.e., sequences richer in K) elute at earlier times in comparison with hydrophilic sequences (i.e., sequences richer in E). A typical example of an RP-HPLC chromatograph obtained for a sample with an initial concentration of tetrapeptide of 200 mg mL^{-1} incubated for 24 h at room temperature and MALDI-TOF MS spectra obtained for the same sample at different incubation times are given in Figure 4. The figure also includes the detailed assignments of the different RP-HPLC and MADLI-TOF MS peaks observed. Sequences with the same number of K and E residues but varying sequential arrangements (e.g., FEFEFKFKK, FEFKFEFK, FEFKFKFE) could not be differentiated as they all have similar overall hydrophobicities and masses. The assignments were confirmed by a combination of
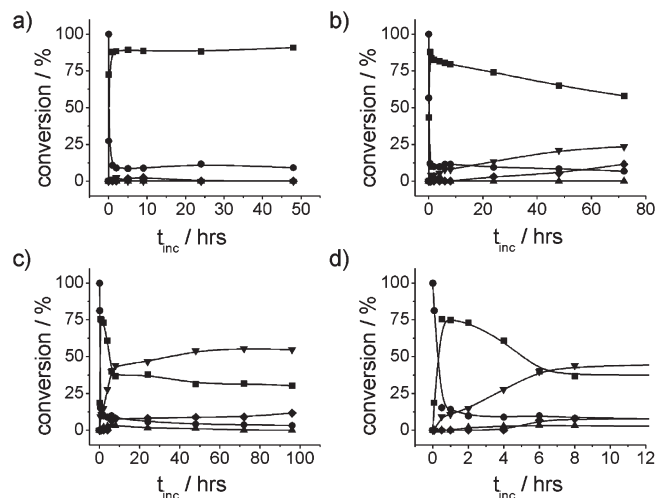
(38) Bowerman, C. J.; Ryan, D. M.; Nissan, D. A.; Nilsson, B. L. *Mol. Biosyst.* **2009**, *5*, 1058−1069.

Figure 5. Evolution of the peptide bond content (conversion %) corresponding to each peptide sequence, di- (■), tetra- (●), hexa- (▲), octa- (▼), and decapeptides (◆) as a function of incubation time for (a) 40, (b) 70, (c and d) 200 mg mL^{-1} samples.

elution times obtained from the RP-HPLC chromatographs of pure peptides, and MALDI-TOF MS results obtained by collecting the sample fractions corresponding to the different HPLC peaks. It should be noted that due to the small mass differences between peptide species with the same number of residues but varying E and K content (e.g., FEFEFEFE and FKFKFKFK molar masses differ by only four units) it was not possible to confirm directly the RP-HPLC peak assignments using only MALDI-TOF MS. Results indicate that both the peptide length and quantities formed over time are dependent on C_0. The evolution of the relative percentages of di-, tetra-, hexa-, octa- and decapeptides for samples with initial concentrations of 40, 70, and 200 mg mL^{-1} are presented in Figure 5 as a function of incubation time (for clarity the percentages given are in peptide bond content corresponding to each peptide sequence). For $C_0 = 40$ mg mL^{-1} (Figure 5a) only di- and tetrapeptides are present after 72 h of incubation. At this concentration hydrolysis of the tetrapeptide occurs and the dipeptides FE and FK are formed as soon as thermolysin is added. After 30 min of incubation the relative quantities of di- and tetrapeptides are 88 and 12%, respectively. It is interesting to note that traces (∼2.5%) of octa- and decapeptides are detected at 1 and 8 h incubation, respectively. This suggests that some reverse-hydrolysis does indeed occur even at low C_0, but these longer sequences disappear with time. It is not clear whether these long sequences are hydrolyzed back to shorter sequences or are extended further. The appearance of decapeptides at a later t_{inc} in comparison to octapeptides would suggest that at least some of the
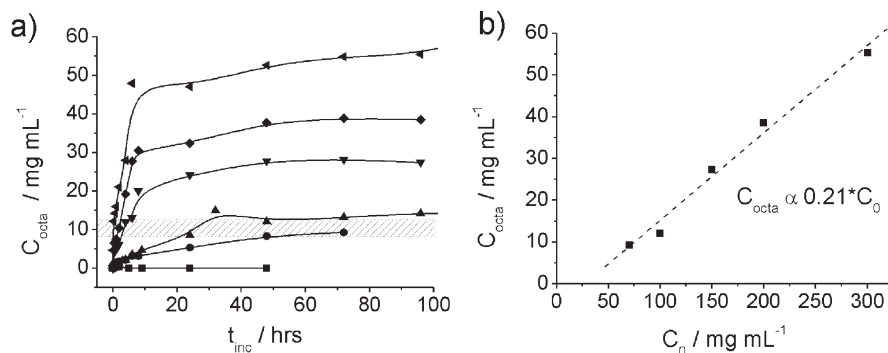
Figure 6. (a) Evolution of the octapeptide concentration (C_{octa} in mg mL^{-1}) as a function of incubation time for 40 (square), 70 (circle), 100 (up triangle), 150 (down triangle), 200 (diamond), and 300 mg mL^{-1} (left triangle) samples; (b) samples' octapeptide concentration after 72 h of incubation vs tetrapeptide initial concentration (C_0 in mg mL^{-1}).

octapeptides are further extended by addition of a dipeptide. For $t_{inc} \geq 10$ h the concentration of di and tetrapeptides is constant suggesting a chemical equilibrium is established, the equilibrium composition of the solution being 10% tetrapeptides and 90% dipeptides.

For $C_0 = 70$ mg mL^{-1} (Figure 5b) the tetrapeptide is hydrolyzed immediately upon the addition of thermolysin, and after 30 min a similar sample composition as the 40 mg mL^{-1} sample is obtained: 88% dipeptides and 12% tetrapeptides. From 30 min onward longer sequences start to form. At $t_{inc} = 2$ h hexa- and octapeptide are both present at the relative concentrations of 3% and 4.5%, respectively. As t_{inc} increases further the quantity of hexapeptides present in the sample is found to decrease until no hexapeptides are detected when $t_{inc} \geq 5$ h. This suggests that hexapeptides are not stable species. In this sample it is also not clear whether the hexapeptides are hydrolyzed back to shorter sequences or undergo reverse hydrolysis and are extended further to form octapeptides, by the addition of a dipeptide, and/or decapeptides, by the addition of a tetrapeptide. The quantity of octapeptides present in the sample is found to increase continuously over the incubation period probed. From 10 h onward decapeptides are also found to form, and their concentration increases continuously during incubation. From $t_{inc} = 5$ h onward the amount of di- and tetrapeptides decreases at a constant rate suggesting that a steady-state reaction is achieved. Even after 72 h no equilibrium is reached. A small, but significant quantity of decapeptides is present in the sample after 72 h. It should be noted that longer species are also likely to form in small quantities. The presence of a very small amount of dodecapeptides was detected by MALDI-TOF MS, although it was not possible to quantify how much was present by HPLC. Various authors have shown that longer peptide sequences based on the same amino acids used here are indeed able to self-assemble and form β-sheet rich fibers.[31,39−42] It is not known whether the decapeptides in our case self-assemble by themselves or co-self-assemble with the octapeptides to form mixed fibers.

For the $C_0 = 200$ mg mL^{-1} sample (Figure 5c and 5d) the tetrapeptide is again hydrolyzed immediately after the addition of thermolysin, and is followed by the formation of longer peptide sequences. In this case the process is significantly faster and after 30 min of incubation 10% of octapeptides are detected along with

75% and 15% di- and tetrapeptides, respectively. From 0.5 to 8 h of incubation a significant increase in octapeptides (up to 44%) and decapeptides (up to 8%) is observed. This increase is accompanied by a sharp decrease in dipeptides (down to 38%) and a slight decrease in tetrapeptides (down to 10%). For this sample hexapeptides are again detected at the early stages (ca. 5−10 h) and then disappear with increasing t_{inc}. From 8 to 48 h a slower increase in octapeptides is observed and from 48 h onward the concentrations of the different peptides species become roughly constant. It is interesting to note, as shown by the HPLC chromatograph presented in Figure 4a, that all the possible octapeptide sequences form during the reverse hydrolysis process, thus creating a combinatorial library of peptide sequences. The sequences formed preferentially are those having the same number of K and E residues (similar results where obtained for the 70 and 100 mg mL^{-1} samples at long incubation times, results not shown). This selectivity in the synthesis process may be related to the solubility and the self-assembling ability of each sequence. For instance the FEFEFEFE sequence is not soluble in water at pH 7 while the FKFKFKFK sequence is soluble but does not self-assemble. The sequences synthesized may also be a reflection of the composition of the sample. In the experiments performed here the number of FE and FK units present is the same at any point in time, and therefore octapeptides containing the same number of K and E residues are statistically more likely to be synthesized. Further work is needed to clarify this point.

Figure 6a summarizes the concentration of octapeptides in mg mL^{-1}, C_{octa}, for each sample as a function of the incubation time. In the figure the concentration range corresponding to the critical gelation concentration, CGC, of FEFEFKFK and FEFKFEFK peptides is also indicated, where these were determined using the "tilting test-tube method" under the same conditions as used here. As can be seen from Figure 6a the macroscopic gelation behavior of our samples correlates well with their overall concentration in octapeptides. For $C_0 = 40$ mg mL^{-1} a small amount of octapeptides form in the early stages (1−2 h of incubation) and subsequently disappears. At such a low octapeptide concentration (< 0.5 mg mL^{-1}) self-assembly is not expected to occur, and this is confirmed by the ATR-FTIR experiments discussed below. For the 70 mg mL^{-1} sample, octapeptides are formed, and the sample viscosity increases with time suggesting that self-assembly occurs in this case. After 1 h of incubation the concentration of octapeptides is ∼2 mg mL^{-1} for this sample. As shown in our previous work self-assembly is indeed expected to occur at this concentration.[36] From 1 h onward the concentration of octapeptides increases suggesting that the self-assembly process thermodynamically stabilizes the octapeptide sequence in preference to

(39) Kopecek, J.; Yang, J. *Acta Biomater* **2009**, *5*, 805−816.
(40) Jun, S.; Hong, Y.; Imamura, H.; Ha, B. Y.; Bechhoefer, J.; Chen, P. *Biophys. J.* **2004**, *87*, 1249−1259.
(41) Hong, Y. S.; Lau, L. S.; Legge, R. L.; Chen, P. *J. Adhes*. **2004**, *80*, 913−931.
(42) Hong, Y. S.; Legge, R. L.; Zhang, S.; Chen, P. *Biomacromolecules* **2003**, *4*, 1433−1442.
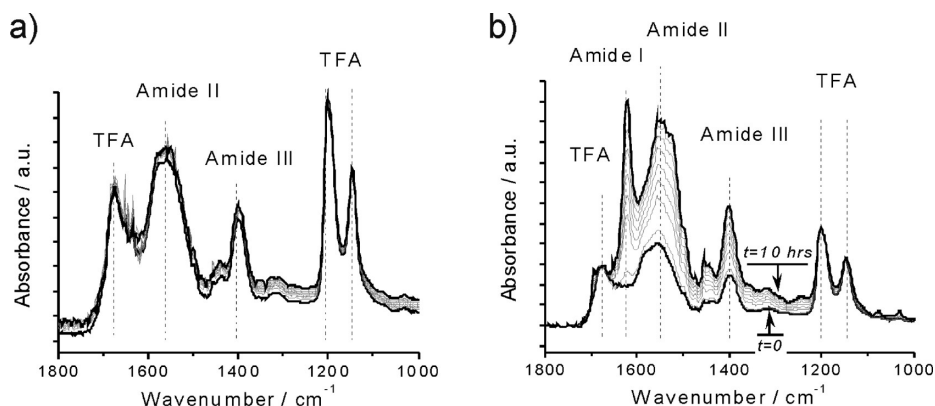
Figure 7. Time-resolved FTIR spectra collected as a function of incubation time for the (a) 40 and (b) 70 mg mL^{-1} samples. Thick black lines correspond to $t = 0$ and 10 h.
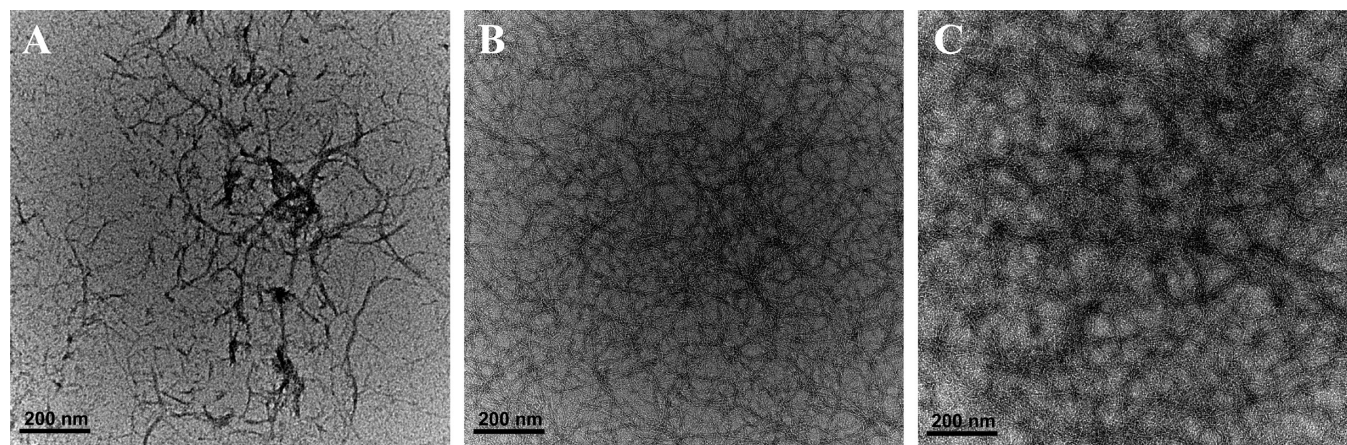

Figure 8. TEM micrographs of undilited 70 (A), diluted 100 (B), and diluted 200 mg mL^{-1} (C) samples after 24 h incubation.

the shorter precursor sequences, namely the tetrapeptide, and results in the chemical equilibrium being shifted toward the production of octapeptides. As tetrapeptides are consumed to synthesize octapeptides, dipeptides are consumed to replace the tetrapeptides creating a chain of interdependent reactions. This is confirmed by the results presented in Figure 5c,d obtained for the 200 mg mL^{-1} sample. The concentration in tetrapeptide remains roughly constant from 2 h onward, and increases in octapeptides concentration correlate with decreases in dipeptide concentration. This is of course a simplistic view of the reactions occurring in our samples. A more complex set of interdependent reactions is expected to occur in which hexa- and decapeptides populations also contribute to the overall dynamics of the sample.

The results obtained for the 40 and 70 mg mL^{-1} samples also suggest that a critical octapeptide concentration (between 0.5 and 2.0 mg mL^{-1}) must be reached before self-assembly, and therefore stabilization of the octapeptides, will occur. The concentration of octapeptides for the 70 mg mL^{-1} sample remains below the CGC of both FEFEFKFK and FEFKFEFK peptides during the entire incubation time probed. This agrees well with the macroscopic behavior of this sample as it increased in viscosity but did not form a self-supporting hydrogel even at long incubation times (up to a week). For samples with $C_0 > 100$ mg mL^{-1} the concentration of octapeptides over time becomes larger than the CGC of FEFEFKFK and FEFKFEFK peptides. This is again in good agreement with the macroscopic behavior observed (Figure 2) for these samples as they were all found to form self-supporting hydrogels over time. These results suggest that the octapeptide is the key peptide sequence that determines sample gelation behavior.

The increase in viscosity and macroscopic gelation of the samples does not seem to affect the enzyme activity. It is evident from Figure 6a that after gelation has occurred, the concentration, and hence the enzymatic synthesis, of octapeptides continues to increase. This is particularly evident for the 300 mg mL^{-1} sample where a macroscopic gel is obtained after ~10 min but the synthesis of octapeptides proceeds at a sustained rate for up to 4−6 h of incubation. After 48−72 h of incubation the concentration of octapeptides for all the samples, whether they are in a gel state or not, becomes roughly constant suggesting an "equilibrium" concentration is reached for this peptide. It should be noted that an overall equilibrium for all different peptide fragments has not been reached after 72 h as shown by the results given in Figure 5. Figure 6b shows the concentration of octapeptides, C_{octa}, after 72 h of incubation as a function of the initial tetrapeptide concentration. It is clear that C_{octa} is proportional to C_0 suggesting that indeed the final concentration of octapeptides obtained corresponds to an "equilibrium" concentration and does not seem to be affected by the gelation of the samples, in good agreement with work performed on short peptide derivatives.[27,28] The slope of the linear fit would then correspond to the conversion constant of initial tetrapeptide into octapeptides (see Figure 6b).

ATR-FTIR and TEM were subsequently used to structurally characterize our samples, that is, to confirm the presence of β-sheet-rich fibers. The ATR-FTIR spectra obtained for the 40 and 70 mg mL^{-1} samples are presented in Figure 7 as a function of the incubation time. The absorption bands observed at 1148, 1200, and 1678 cm^{-1} are due to the presence of residual

TFA in our original peptide sample. As the concentration of TFA is constant for a given sample, and proportional to C_0 (all the samples were prepared using the same batch of tetrapeptide), the band at 1148 cm^{-1} was used to normalize all ATR-FTIR spectra. The absorption bands at 1400 and 1555 cm^{-1} correspond to the amide II and amide III bands, respectively. The intensities of these two absorption bands increase significantly for the 70 mg mL^{-1} sample (Figure 7b) due to the creation of amide bonds resulting from the synthesis of octa- and decapeptides. In addition for this sample a strong band at 1622 cm^{-1} and a weaker band at 1693 cm^{-1} appear and grow with increasing t_{inc}. Similar results were obtained for samples with higher C_0 (results not shown). These bands have previously been assigned to peptides adopting an antiparallel β-sheet arrangement.[43,44] The TEM micrographs obtained for the 70, 100, and 200 mg mL^{-1} samples after 24 h of incubation are presented in Figure 8. As can be seen fibrils are observed in all cases. The diameters of all fibers are ca. 3–6 nm, which is similar to those we obtained previously for pure octapeptide hydrogels.[35,36] These results suggest that for $C_0 \geq 70$ mg mL^{-1} self-assembly of the peptide does indeed occur and antiparallel β-sheet rich fibrils form. For the 70 mg mL^{-1} sample isolated fibrillar aggregates are observed and no extended 3D network of fibers is ever observed, even at longer incubation times (up to a week). This is in good agreement with our observation that no macroscopic gel is formed for this sample. In contrast, extended 3D networks of entangled fibers are observed for the 100 and 200 mg mL^{-1} samples, which is in agreement with our visual observation of the formation of macroscopic hydrogels. No fibrils were observed for the 40 mg mL^{-1} sample by TEM, and the absorption bands at 1622 and 1693 cm^{-1} are absent from the ATR-FTIR spectra (Figure 7a) even at early incubation times when a limited amount of octapeptides were observed to form. This confirms that the concentration of octapeptides attained in this sample is below the critical self-assembling concentration.

Conclusions

In this paper we have investigated the possibility of using the protease thermolysin to trigger the reverse-hydrolysis and sub-sequent gelation of ionic-complementary peptides. Thermolysin was added at a fixed concentration (0.3 mg mL^{-1}) to aqueous solutions (0–300 mg mL^{-1}) of a short tetrapeptide (FEFK). The simultaneous analysis of MALDI-TOF MS and RP-HPLC chromatographs as a function of incubation time allowed the composition of the system to be elucidated, and it was found that different peptide sequences formed depending on the initial concentration of tetrapeptides, C_0. For all samples the protease initially hydrolyzed the tetrapeptides into the dipeptides FE and FK. Subsequently longer peptide sequences (hexa-, octa-, and decapeptides) were found to form through reverse-hydrolysis. At low C_0 (< 70 mg mL^{-1}) these longer sequences were found to be unstable and disappeared with increasing incubation time. As C_0 was increased (≥ 70 mg mL^{-1}) the octapeptide became the dominant product of the reverse-hydrolysis reaction. As the quantity of octapeptide synthesized increased, self-assembly into antiparallel β-sheet-rich fibers was observed, as confirmed by ATR-FTIR and TEM. Our results suggest that a critical self-assembly concentration for the octapeptide was required (ca. 0.5–2 mg mL^{-1}). When at, and above, this critical concentration, self-assembly occurred and resulted in the thermodynamic stabilization of the peptide in preference to its shorter precursors. The self-assembling property of the octapeptides was found to be key to their stabilization. For example hexapeptides were also found to form, but this peptide does not self-assemble at such low concentrations, therefore, it was not found to be a stable sequence as it always disappeared with increasing incubation time. At long incubation times (> 72 h) the concentration of octapeptides leveled off and was directly proportional to C_0, suggesting that some type of "equilibrium" concentration was reached for this peptide. Moreover the octapeptide concentration was found to dictate the gelation behavior of the samples. At high C_0 (≥ 100 mg mL^{-1}) the concentration of octapeptide synthesized became higher than the critical gelation concentration of pure octapeptides and resulted in the formation of self-supporting hydrogels. Gels with moduli up to 25 kPa where obtained depending on C_0.

This novel method of forming ionic peptides, and subsequently hydrogels, will undoubtedly have significant impact in the synthesis of longer peptides and will also find important applications for the formation of scaffolds for in vivo tissue engineering or for enzyme detection.

(43) Barth, A. *Biochim. Biophys. Acta, Bioenerg.* **2007**, *1767*, 1073–1101.
(44) Barth, A.; Zscherp, C. *Q. Rev. Biophys.* **2002**, *35*, 369–430.